REPORT DOCUMENTATION PAGE

Form Approved OMB NO. 0704-0188

1. REPORT DATE (DD-MM-YYYY)	2. REPORT TYPE	3. DATES COVERED (From - To)
31-08-2015	Final Report	1-Sep-2014 - 31-May-2015

4. TITLE AND SUBTITLE
Final Report: Design and Development of Electrically Pumped Coaxial Nanoscale Laser for On-chip Optical Communication - TOPIC STIR

5a. CONTRACT NUMBER
W911NF-14-1-0543

5b. GRANT NUMBER

5c. PROGRAM ELEMENT NUMBER
611102

6. AUTHORS
Mercedeh Khajavikhan, Patrick LiKamWa

5d. PROJECT NUMBER

5e. TASK NUMBER

5f. WORK UNIT NUMBER

7. PERFORMING ORGANIZATION NAMES AND ADDRESSES
University of Central Florida
12201 Research Parkway, Suite 501

Orlando, FL 32826 -3246

8. PERFORMING ORGANIZATION REPORT NUMBER

9. SPONSORING/MONITORING AGENCY NAME(S) AND ADDRESS (ES)
U.S. Army Research Office
P.O. Box 12211
Research Triangle Park, NC 27709-2211

10. SPONSOR/MONITOR'S ACRONYM(S)
ARO

11. SPONSOR/MONITOR'S REPORT NUMBER(S)
66280-EL-II.11

12. DISTRIBUTION AVAILIBILITY STATEMENT
Approved for Public Release; Distribution Unlimited

13. SUPPLEMENTARY NOTES
The views, opinions and/or findings contained in this report are those of the author(s) and should not contrued as an official Department of the Army position, policy or decision, unless so designated by other documentation.

14. ABSTRACT
Small footprints, low power consumption, and high operating speeds are some of the desirable attributes of future chip-scale photonic integrated circuits (PIC). This has fueled some of the recent activities in developing nanolasers as one of the key components of such integrated systems. To overcome the challenges facing laser miniaturization, drastically new designs based on metallic nano-cavities have been pursued. Along these lines, optically pumped nanolasers based on a metallic coaxial architecture, as well as electrically pumped nanolasers utilizing metallo-

15. SUBJECT TERMS
semiconductor lasers, nanolasers, coaxial lasers

16. SECURITY CLASSIFICATION OF: a. REPORT	b. ABSTRACT	c. THIS PAGE	17. LIMITATION OF ABSTRACT	15. NUMBER OF PAGES	19a. NAME OF RESPONSIBLE PERSON
UU	UU	UU	UU		Mercedeh Khajavikhan
					19b. TELEPHONE NUMBER 407-823-6829

Standard Form 298 (Rev 8/98)
Prescribed by ANSI Std. Z39.18

Report Title

Final Report: Design and Development of Electrically Pumped Coaxial Nanoscale Laser for On-chip Optical Communication - TOPIC STIR

ABSTRACT

Small footprints, low power consumption, and high operating speeds are some of the desirable attributes of future chip-scale photonic integrated circuits (PIC). This has fueled some of the recent activities in developing nanolasers as one of the key components of such integrated systems. To overcome the challenges facing laser miniaturization, drastically new designs based on metallic nano-cavities have been pursued. Along these lines, optically pumped nanolasers based on a metallic coaxial architecture, as well as electrically pumped nanolasers utilizing metallo-dielectric structures were demonstrated in the past. In the course of this STIR project, the PIs performed a feasibility study for developing electrically pumped coaxial nano-lasers that could be effectively coupled to a silicon interconnect via a plasmonic waveguide section. To this end, lasing has been demonstrated in coaxial nanolasers fabricated on wafers capable of becoming electrically pumped. A rate equation model is developed to calculate the lasing threshold as well as the highest possible speed for such devices under optical pumping. Effort also has been directed towards accurately measuring the second order coherence function of optically pumped nanolasers.

Enter List of papers submitted or published that acknowledge ARO support from the start of the project to the date of this printing. List the papers, including journal references, in the following categories:

(a) Papers published in peer-reviewed journals (N/A for none)

Received Paper

TOTAL:

Number of Papers published in peer-reviewed journals:

(b) Papers published in non-peer-reviewed journals (N/A for none)

Received Paper

TOTAL:

Number of Papers published in non peer-reviewed journals:

(c) Presentations

1- W. Hayenga, M. Khajavikhan, “Rate Equation Analysis of High-Speed Nanolasers”, SPIE Photonics West San Francisco CA (2015)

2- H. Hodaei, M. A. Miri, M. Heinrich, D. Christodoulides, M. Khajavikhan, “PT-symmetric microring lasers”, SPIE Photonics West San Francisco CA (2015)

3-M. Khajavikhan, "Metallic and Metallo-Dielectric Coaxial Nanolasers", IEEE Summer Topicals, Bahamas (2015)

Number of Presentations: 3.00

Non Peer-Reviewed Conference Proceeding publications (other than abstracts):

Received	Paper

TOTAL:

Number of Non Peer-Reviewed Conference Proceeding publications (other than abstracts):

Peer-Reviewed Conference Proceeding publications (other than abstracts):

Received		Paper
08/27/2015	3.00	Hossein Hodaei, William Hayenga, Mercedeh Khajavikhan, Absar Hassan, Demetrios Christodoulides. Enhanced Sensitivity in Parity-Time-Symmetric Microcavity Sensors, Optical Sensors. 30-JUN-15, Boston, Massachusetts. : ,
08/27/2015	4.00	Hossein Hodaei, William Hayenga, Mohammad-Ali Miri, Absar Ulhassan, Demetrios N. Christodoulides, Mercedeh Khajavikhan. Dark state microring lasers: Using non-Hermitian exceptional points for mode management, CLEO: Applications and Technology. 07-JUN-15, San Jose, California. : ,
08/27/2015	5.00	William Hayenga, Mohammad-Ali Miri, Hossein Hodaei, Absar Ulhassan, Mathias Heinrich, Demetrios N. Christodoulides, Mercedeh Khajavikhan. Single Mode Broad Area PT-Symmetric Microring Lasers, CLEO: QELS_Fundamental Science. 07-JUN-15, San Jose, California. : ,
08/27/2015	7.00	Hossein Hodaei, William Hayenga, Mohammad-Ali Miri, Absar Ulhassan, Demetrios N. Christodoulides, Mercedeh Khajavikhan. Tunable Parity-Time-Symmetric Microring Lasers, CLEO: Science and Innovations. 07-JUN-15, San Jose, California. : ,

TOTAL: **4**

Number of Peer-Reviewed Conference Proceeding publications (other than abstracts):

(d) Manuscripts

Received		Paper
08/25/2015	1.00	H. Hodaei, M.-A. Miri, M. Heinrich, D. N. Christodoulides, M. Khajavikhan. Parity-time-symmetric microring lasers, Science (10 2014)
08/27/2015	10.00	M. Ali Miri, W. Hayenga, A. Ulhassan, D.N. Christodoulides, M. Khajavikhan, Hossein Hodaei. Dark state microring lasers:Mode management using exceptional points, Nature Photonics (03 2015)
08/27/2015	8.00	Hossein Hodaei, Mohammad Ali Miri, Absar Ulhassan, William Hayenga, Matthias Heinrich, Demetrios N. Christodoulides, Mercedeh Khajavikhan. Parity-time-symmetric coupled microring lasers operating around an exceptional point, Optics Letters (07 2015)
08/27/2015	9.00	Hossein Hodaei, M. Ali Miri, William Hayenga, Absar Ulhassan, Matthias Heinrich, Demetrios N. Christodoulides, Mercedeh Khajavikhan. Single mode lasing in transversely multi-moded PTsymmetricmicroring resonators, Optica (07 2015)

TOTAL: **4**

Number of Manuscripts:

Books

Received	Book

TOTAL:

Received Book Chapter

TOTAL:

Patents Submitted

N/A

Patents Awarded

N/A

Awards

N/A

Graduate Students

NAME	PERCENT_SUPPORTED	Discipline
William Hayenga	0.57	
Hossein Hodaei	0.15	
FTE Equivalent:	**0.72**	
Total Number:	**2**	

Names of Post Doctorates

NAME	PERCENT_SUPPORTED
N/A	0.00
FTE Equivalent:	**0.00**
Total Number:	**1**

Names of Faculty Supported

NAME	PERCENT_SUPPORTED	National Academy Member
Mercedeh Khajavikhan	0.00	
Patrick Likamwa	0.00	
FTE Equivalent:	**0.00**	
Total Number:	**2**	

Names of Under Graduate students supported

NAME	PERCENT_SUPPORTED	Discipline
N/A	0.00	
FTE Equivalent:	**0.00**	
Total Number:	**1**	

Student Metrics

This section only applies to graduating undergraduates supported by this agreement in this reporting period

The number of undergraduates funded by this agreement who graduated during this period: 0.00

The number of undergraduates funded by this agreement who graduated during this period with a degree in science, mathematics, engineering, or technology fields:...... 0.00

The number of undergraduates funded by your agreement who graduated during this period and will continue to pursue a graduate or Ph.D. degree in science, mathematics, engineering, or technology fields:...... 0.00

Number of graduating undergraduates who achieved a 3.5 GPA to 4.0 (4.0 max scale):...... 0.00

Number of graduating undergraduates funded by a DoD funded Center of Excellence grant for Education, Research and Engineering:...... 0.00

The number of undergraduates funded by your agreement who graduated during this period and intend to work for the Department of Defense 0.00

The number of undergraduates funded by your agreement who graduated during this period and will receive scholarships or fellowships for further studies in science, mathematics, engineering or technology fields:...... 0.00

Names of Personnel receiving masters degrees

NAME	
N/A	
Total Number:	**1**

Names of personnel receiving PHDs

NAME	
N/A	
Total Number:	**1**

Names of other research staff

NAME	PERCENT_SUPPORTED
N/A	0.00
FTE Equivalent:	**0.00**
Total Number:	**1**

Sub Contractors (DD882)

1 a. N/A

1 b.

00000

Sub Contractor Numbers (c):

Patent Clause Number (d-1):

Patent Date (d-2):

Work Description (e):

Sub Contract Award Date (f-1):

Sub Contract Est Completion Date(f-2):

Inventions (DD882)

Scientific Progress

Technology Transfer

N/A

Small footprints, low power consumption, and high operating speeds are some of the desirable attributes of future chip-scale photonic integrated circuits (PIC) [1]. This has fueled some of the recent activities in developing nanolasers as one of the key components of such integrated systems. To overcome the challenges facing laser miniaturization, drastically new designs based on metallic nano-cavities have been pursued [2-14]. Along these lines, optically pumped nanolasers based on a metallic coaxial architecture [13], as well as electrically pumped nanolasers utilizing metallo-dielectric structures were demonstrated in the past [11]. In the course of this STIR project, the PIs performed a feasibility study for developing electrically pumped coaxial nano-lasers that could be effectively coupled to a silicon interconnect via a plasmonic waveguide section. To this end, lasing has been demonstrated in coaxial nanolasers fabricated on wafers capable of becoming electrically pumped. A rate equation model is developed to calculate the lasing threshold as well as the highest possible speed for such devices under optical pumping. Effort also has been directed towards accurately measuring the second order coherence function of optically pumped nanolasers.

Rate equation model

Due to plasmonic properties of metals at optical frequencies, metallic cavities can support highly confined sub-wavelength modes. Such ultra-small mode volumes, unique to this family of resonators, has important ramifications in nanolaser design in several aspects including high mode confinement (Γ), large Purcell factor (F), and under certain circumstances, close to unity spontaneous emission coupling factor (β). The role of these parameters in improving the frequency response as well as in reducing the lasing threshold, despite the inherent lossy nature of metallic cavities, can be explained through the following rate equations representing the laser dynamics,

$$\begin{cases} \frac{dn_p}{dt} = \frac{F}{\tau_{sp}}\left(\frac{\Gamma\gamma^{-1}}{1+\frac{\epsilon}{V_{eff}}n_p}n_p + \Gamma\beta\right)n_c - \frac{n_p}{\tau_p} \\ \frac{dn_c}{dt} = \frac{I}{e} - \frac{F}{\tau_{sp}}\left(\frac{\gamma^{-1}}{1+\frac{\epsilon}{V_{eff}}n_p}n_p + 1\right)n_c - \frac{n_c}{\tau_{nr}} \end{cases} \quad \text{(Eq. 1).}$$

In the above coupled system of equations, n_c and n_p are the total number of electron–hole pairs in the active region and photons in the lasing mode respectively, τ_{sp} is the bulk upper state lifetime, τ_{nr} is the non-radiative lifetime, τ_p is the photon lifetime of the cavity, $\gamma \cong f_c(1-f_v)/(f_c - f_v)$, where f_c and f_v are the Fermi-Dirac function in the conduction and valence bands, respectively, I is the injection current, e is the charge of the electron, and ϵ is the gain suppression coefficient. The Purcell factor (F) is defined as the ratio of the rate of spontaneous emission in bulk to cavity and is given by $(3/4\pi^2)\,(\lambda_c/n)^3\,(\min\{Q, Q_h\}/(V_{eff})$, where Q_h is the quality factor representing the homogenous linewidth of the gain material and Q is the quality factor of the cavity, and V_{eff} is the mode volume. The spontaneous emission coupling factor β is defined as the ratio of spontaneous emission into the lasing mode to the total spontaneous emission [15-19].

It should be noted that the above treatment departs from some of the recently published rate equation models for nanolasers. For example, in some of the previous works the effect of mode confinement is ignored (needless to emphasize high mode confinement is one of the key features of metal-cavity lasers), and in some others the effect of the cavity in modifying the stimulated emission is neglected (the Purcell factor is only applied to spontaneous emission, therefore more

stringent pumping and quality factors were falsely required for stimulated emission to become the dominant photon generating process) [20,21].

From the above rate equations, the relaxation oscillation frequency and the damping coefficient can be obtained by differentiating the steady state to find $\mathcal{H}(\nu) = \nu_r^2/(\nu_r^2 - \nu^2 - i\zeta\nu)$ (the normalized modulation transfer function) in which ν_r is the relaxation oscillation frequency and ζ is the damping coefficient.

$$\nu_r = \frac{1}{2\pi}\sqrt{\begin{array}{l} [\frac{F}{\tau_{sp}}\frac{\gamma^{-1}}{1+\frac{\epsilon}{V_{eff}}n_{p_o}}(\frac{\epsilon}{V_{eff}}\frac{n_{p_o}n_{c_o}}{1+\frac{\epsilon}{V_{eff}}n_{p_o}}+1)]\ (\frac{n_{p_o}\gamma^{-1}}{1+\frac{\epsilon}{V_{eff}}n_{p_o}}+\frac{F\Gamma\beta}{\tau_{sp}}) \\ +[\frac{1}{\tau_p}-\frac{F\Gamma}{\tau_{sp}}\frac{\epsilon}{V_{eff}}\frac{n_{c_o}\gamma^{-1}}{1+\frac{\epsilon}{V_{eff}}n_{p_o}}(\frac{n_{p_o}}{1+\frac{\epsilon}{V_{eff}}n_{p_o}}-1)][\frac{F}{\tau_{sp}}(\frac{n_{p_o}\gamma^{-1}}{1+\frac{\epsilon}{V_{eff}}n_{p_o}}+1)+\frac{1}{\tau_{nr}}] \end{array}}$$

$$\zeta = \frac{1}{2\pi}\{[\frac{F}{\tau_{sp}}(\frac{n_{p_o}\gamma^{-1}}{1+\frac{\epsilon}{V_{eff}}n_{p_o}}+1)+\frac{1}{\tau_{nr}}]+[\frac{1}{\tau_p}-\frac{F\Gamma}{\tau_{sp}}\frac{\epsilon}{V_{eff}}\frac{n_{c_o}\gamma^{-1}}{1+\frac{\epsilon}{V_{eff}}n_{p_o}}(\frac{n_{p_o}\gamma^{-1}}{1+\frac{\epsilon}{V_{eff}}n_{p_o}}+1)]\} \qquad \text{(Eq. 2)}$$

The modulation bandwidth $\nu_{FWHM} = \mathrm{sqrt}((\sqrt{4\nu_r^4 + \zeta^4} - \zeta^2)/2)$ will then be found by setting $\Re\{\mathcal{H}(\nu)\} = 1/2$. In Fig. 1a and b the modulation bandwidth is plotted as a function of injection current for several cavity sizes and quality factors. As can be seen, unprecedentedly larger bandwidths are within reach using metallic arrangements with ultra-small mode volumes– potentially eliminating the need for independent on-chip modulators.

The above analysis not only confirms what has been conjectured about the large modulation bandwidth of nanolasers, but also shows the extent of it. In particular it shows how cavity parameters (quality factor and volume) affect the bandwidth. From this analysis, it is clear that as expected lowering Q and reducing the volume will enhance the modulation response of nanolasers.

The question that remained to be addressed here is whether or not the lasing is achieved under such low pump powers in the metallic cavities with low quality factors and small mode volumes [15-22]. From the rate equations in (1), under steady state conditions, the carrier density as well as the photon density in the lasing mode as a function of the steady state current (I_0) are expressed by:

$$n_{c_o} = \frac{n_{p_o}\tau_{sp}(1+\frac{\epsilon}{V_{eff}}n_{p_o})}{\tau_p F\Gamma n_{p_o}\gamma^{-1}+\beta(1+\frac{\epsilon}{V_{eff}}n_{p_o})}$$

$$n_{p_o} = \frac{1}{2(F\tau_{nr}(V_{eff}+\gamma\epsilon)+\gamma\epsilon\tau_{sp})}\{-(V_{eff}\gamma(F\tau_{nr}+\tau_{sp}) - F\frac{I_o}{e}\Gamma\tau_{nr}\tau_p(V_{eff}+\beta\gamma\epsilon)) + \sqrt{(V_{eff}\gamma(F\tau_{nr}+\tau_{sp}) - F\frac{I_o}{e}\Gamma\tau_{nr}\tau_p(V_{eff}+\beta\gamma\epsilon))^2 + 4F\frac{I_o}{e}V_{eff}\beta\gamma\Gamma\tau_{nr}\tau_p(F\tau_{nr}(V_{eff}+\gamma\epsilon)+\gamma\epsilon\tau_{sp})}\} \qquad \text{(Eq.3)}$$

In order to discern the lasing threshold, where the stimulated emission overcomes the spontaneous emission, The first equation in (1) has been broken up into the part accountable for the stimulated emission ($\boldsymbol{\frac{F}{\tau_{sp}}\Gamma\gamma^{-1}(1+\frac{\epsilon}{V_{eff}}n_{p_o})^{-1}n_{p_o}n_{c_o}}$), and the part representing the spontaneous emission ($\boldsymbol{\frac{F}{\tau_{sp}}\Gamma\beta n_{c_o}}$). Figure 2 shows the combinations of the spontaneous power and the stimulated emitted power for varying cavity sizes and quality factors. This simple analysis clearly shows that lossy metal cavities with smaller mode volumes are in fact capable of sustaining lasing oscillations despite their considerably lower quality factors. However as the loss increases above a certain value, the smaller mode volume no longer lowers threshold.

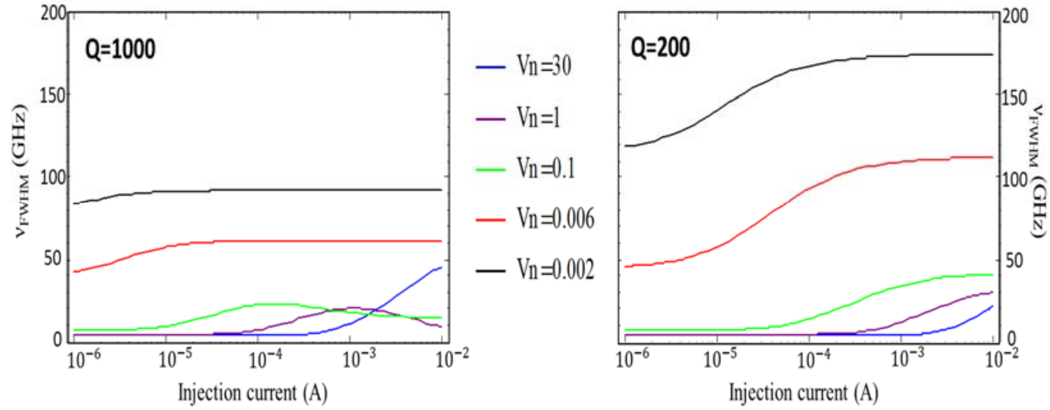

Figure 2 a) the modulation response is plotted for a Q of 1000 and the response is plotted for various cavity sizes. It is seen that as the cavity size decreases that the modulation response increases, 9b) displays the modulation response with a Q=200, resulting in an increased modulation bandwidth. The following parameters were used when calculating the plots: λ_0=1542 nm, n=3.4,τ_{nr}= 40 ps, τ_{sp}= 4 ns, γ=4, τ_p= Q/(2πc/ λ_0), Γ=0.2, V_n=$V_{eff}/(\lambda/2n)^3$, β=0.41, and ϵ=2.3e-23 m^3.

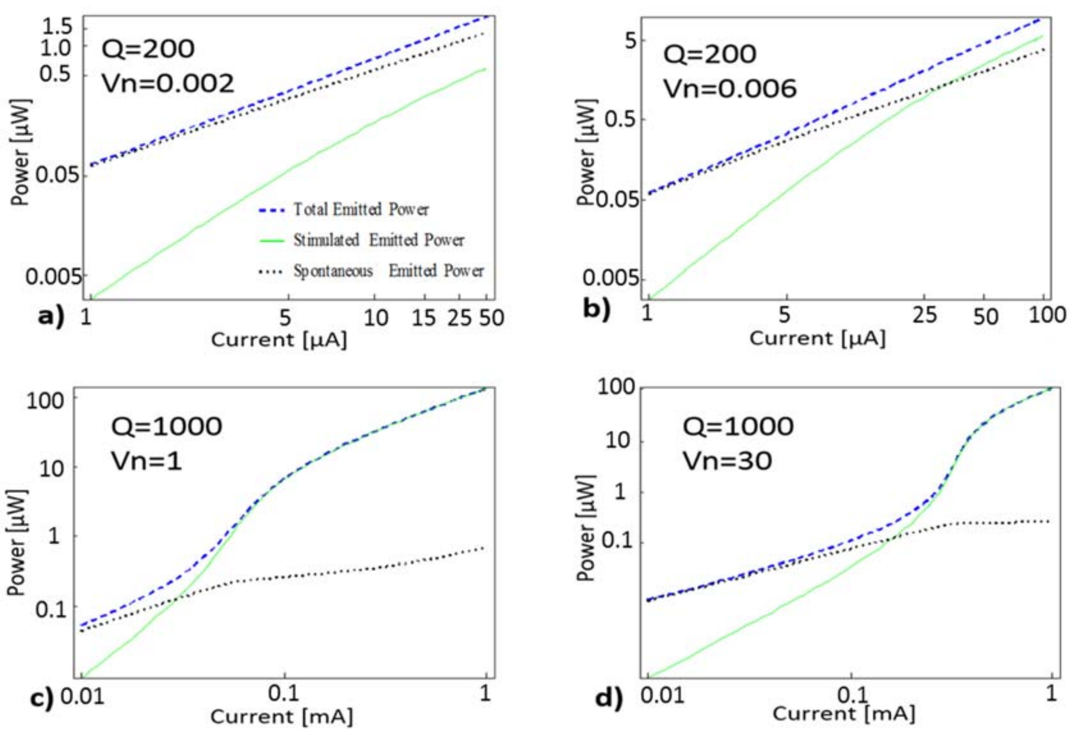

Figure 1 **(a) Q=200 and V_n=0.002. Due to the small cavity size, the spontaneous emission is always larger than the stimulated emission and the device will not lase. (b) The cavity size is increased to V_n=0.006, while Q=200, resulting in stimulated emission overcoming the spontaneous emission. (c) The cavity size and the quality factory are both increased to Q=1000 and V_n=1. The increase in V_n causes the threshold to increase, while the increase in the quality factor causes the threshold to decrease, consequentially the lasing threshold is comparable to the device in plot (b). (d) Here Q=1000 and V_n=30. The increase in the cavity size while keeping *Q* the same as that in plot (c) clearly demonstrates the importance of cavity size on lowering the lasing threshold.**

Optically pumped coaxial nanolaser using a wafer designed for electrical pumping

The feasibility of electrically pumped (EP) nanoscale coaxial lasers is examined by testing such lasers under optical pumping. Figure 3 shows the specs of the EP wafer, and the resulting emission spectra from a coaxial structure with an inner radius of a 100 nm and an outer radius of a 300 nm. The total thickness of the semiconductor part of the structure is 475 nm [23].

Layer #	Material	Thickness (Å)	Loop	Dopant	Comment
10	InGaAs	500	1	Si (n ~ 2E19 cm-3)	lattice-matched
9	InP	500	1	Si (n ~ 5E18 cm-3)	
8	InP	500	1	Si (n ~ 1E18 cm-3)	
7	1.3 Q $In_xGa_{1-x}As_yP_{1-y}$	200	6	undoped	x=0.734, y=0.571
6	1.6 Q $In_xGa_{1-x}As_yP_{1-y}$	100	6	undoped	x=0.560, y=0.938
5	1.3 Q $In_xGa_{1-x}As_yP_{1-y}$	200	1	undoped	x=0.734, y=0.571
4	InP	500	1	Zn (p ~ 1E18 cm-3)	
3	InP	750	1	Zn (p ~ 5E18 cm-3)	
2	InGaAsP 1.24Q	500	1	Zn (p ~ 2E19 cm-3)	lattice-matched
1	InP	1000	1	undoped	
0	2" i-InP DSP (100)			undoped	Substrate
	Total thickness (um)	0.625			

(a)

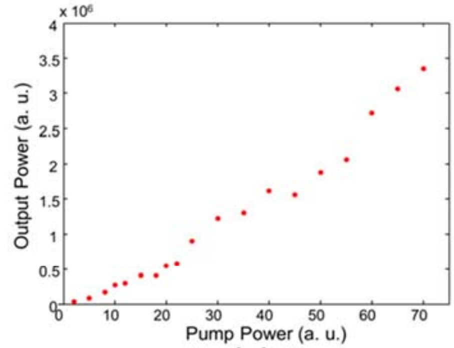

(c)

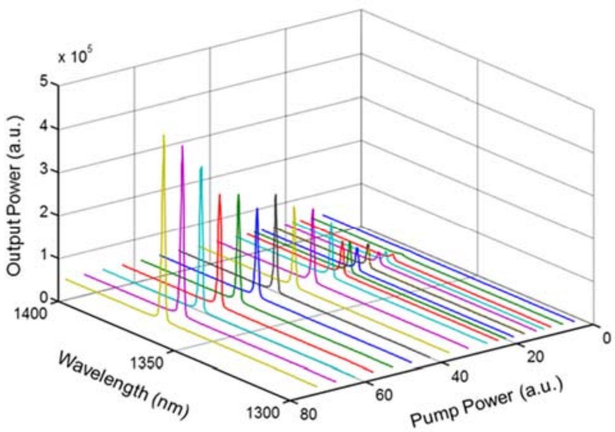

(b)

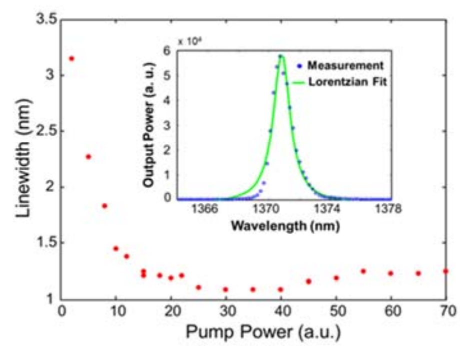

(d)

Figure 3 (a) layer specification of the wafer designed and epitaxially grown for fabricating electrically pumped coaxial nanolasers. (b) the spectral evolution of the emitted radiation from a coaxial structure with an inner radius of a 100 nm, an outer radius of a 300 nm, and the total height of 475 nm, (c) the output power and (d) the linewidth vs. the pump power. The inset in (d) shows the Lorentzian fit to the measured data.

Second-order coherence ($g^{(2)}$) measurement

A $g^{(2)}$ measurement capability is established at CREOL for characterizing nanoscale lasers operating at 900 nm to 1700 nm wavelength regime. The $g^{(2)}$ measurement can unambiguously determine the nature of the emitted light (chaotic, coherent, or quantum). In addition, it provides an in-depth understanding of the mechanisms leading to light generation in such nanoscale cavities. This knowledge in turn may be used to design more efficient light sources. Figure 4a depicts the schematic of the $g^{(2)}$ set-up integrated with the micro-photo-luminescence measurement station [24-25].

The above set-up has been used to characterize a number of nanoscale light sources based on disks of different radii covered with metallic claddings. The metal-clad disk cavity is selected because it generates relatively high power (in some cases larger than 50 μW of power is collected using a power meter). The metallic cladding and the removal of the dielectric shield were also instrumental in operating these nanolasers under CW optical pumping. Figure 5 shows the $g^{(2)}$ measurement result for a nanolaser of a radius of 700 nm, along with light-light and

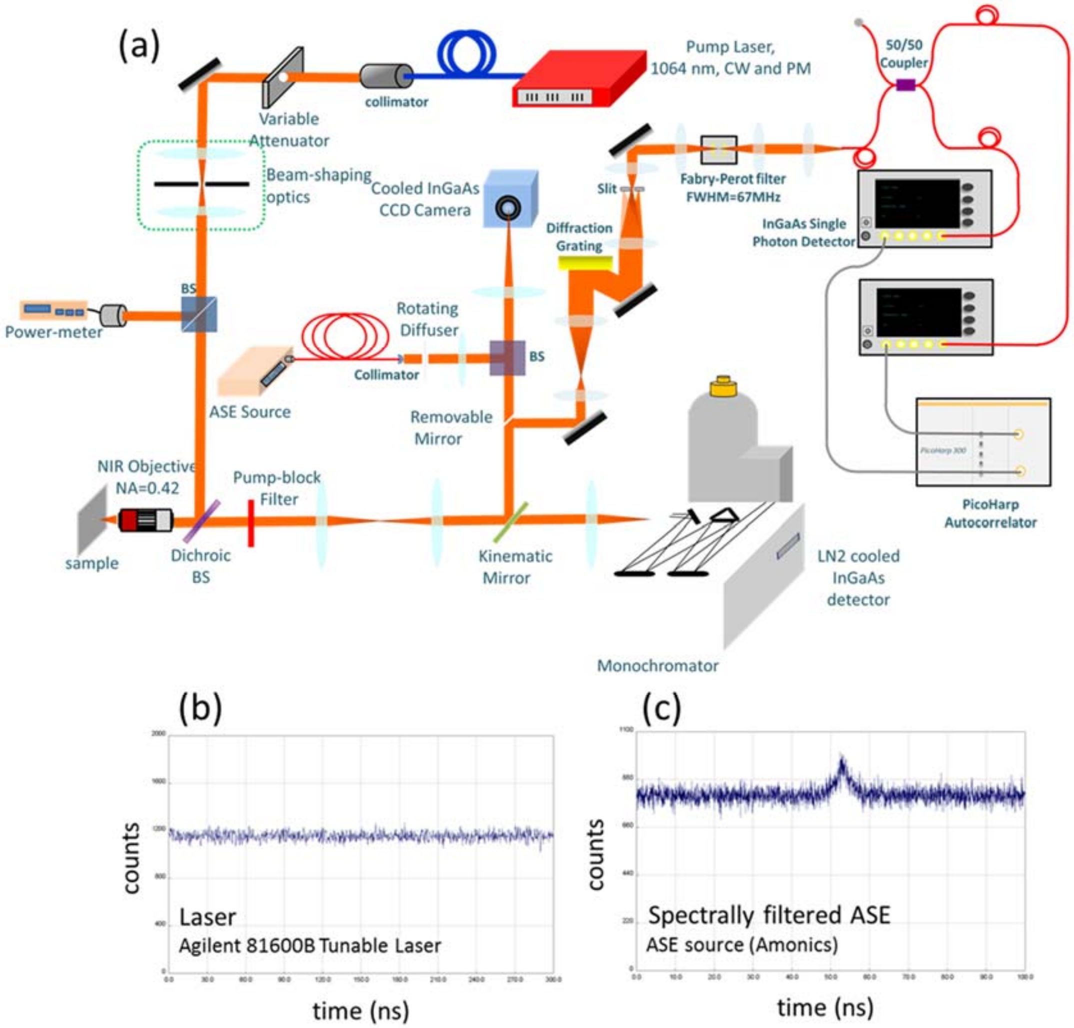

Figure 4 (a) Schematic of the $g^{(2)}$ set-up integrated in the micro-photo-luminescence measurement station. (b) The second-order correlation measurement of an Agilent 81600B Tunable laser and (c) a spectrally filtered ASE source. The ASE source has a clear peak at $g^{(2)}(0)$ (corresponding to 57 ns), a result of chaotic light, while the laser displays no marked features.

linewidth characterization. While the logarithmic light-light curve clearly shows an S-shape, the linewidth slowly increases above threshold and so does the maximum of the $g^{(2)}$ value at zero time delay (corresponding to 50 ns in Fig. 5c).

It should be noted that even though each of the single photon counters require less than 50Kcount/s (corresponding to a power 1.6e-14 Watt), several issues have prevented from measuring $g^{(2)}$ below lasing threshold (especially at PL regime):

1) Mode profile mismatch between the nanolasers (collected with a high numerical aperture objective) and the single mode fiber.
2) Low detection efficiency of single photon counters and high dark counts level (1Kc/s to 2Kc/s at 5% efficiency and 20μs dead-time)

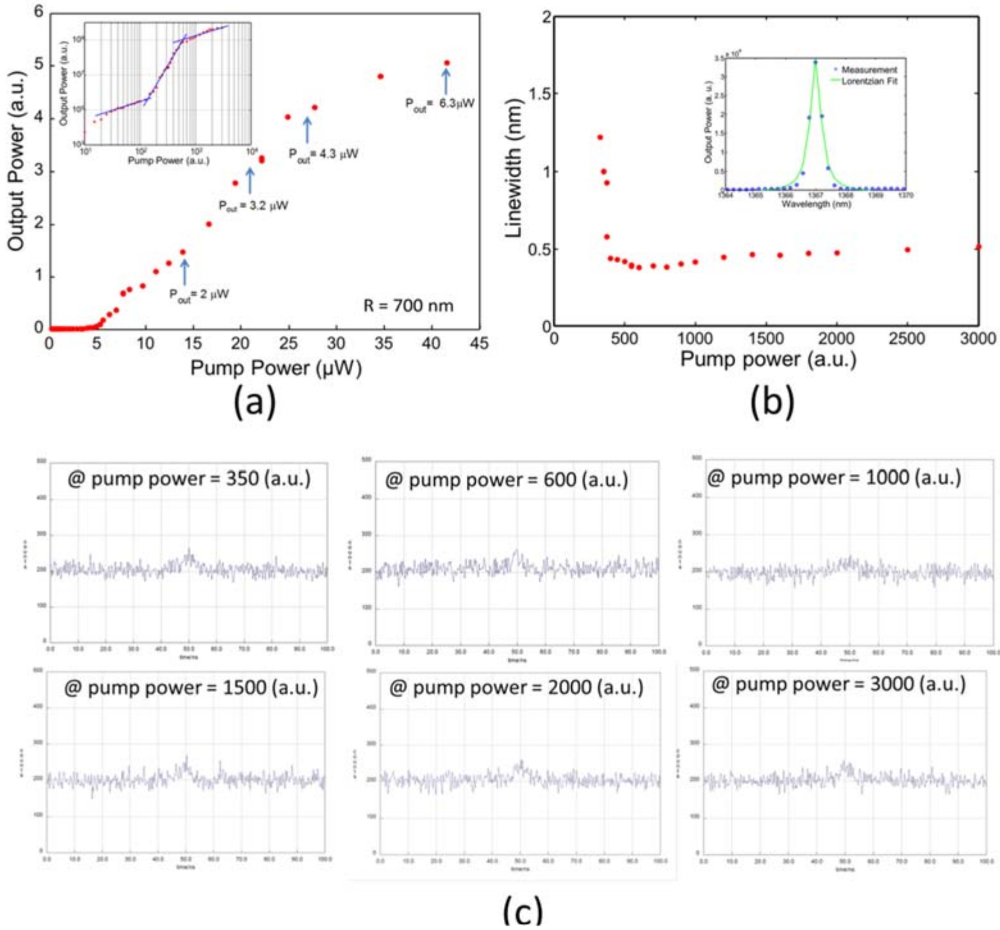

Figure 5 (a) light-light curve and (b) linewidth vs. pump power for a metal-clad disk structure with a radius of 700 nm. In (c) the $g^{(2)}$ measurement result is provided at different pump power levels corresponding to points in ASE and lasing sections of light-light curve. All $g^{(2)}$ measurements are performed under CW pumping and at the count rate of 25Kc/s. The first channel has an offset of -50 ns. The inset in (a) and (b) shows the light-light curve in the log-log scale and the Lorentzian fit to the measured linewidth, respectively

3) The low timing resolution (200 ps) of the single photon counters and the large emission linewidth of nanolasers (approximately 1 nm that should be externally narrowed down to 0.0005 nm, this results in a ~15 ns coherence time).

Some of these issues will be automatically resolved by moving to a wavelength of ~980 nm where silicon based single photon counters (low dark count and short timing resolution) can be utilized We are also currently in negotiation with ID Quantique (http://www.idquantique.com/) to exchange our single photon counters (ID210) with their new model which has lower dark count and higher efficiency (ID220).

The observed fluctuation can also indicate excess relative intensity noise (RIN) generated by the fluctuations of the pump power as well as the mechanical vibrations in the set-up. More accurate G^2 measurement will become possible once the electrically pumped nanolasers are developed using low noise current sources.

Bibliography

1. Q. Gu, J. ST Smalley, M. P. Nezhad, A. Simic, J. H. Lee, M. Katz, O. Bondarenko, B. Slutsky, A. Mizrahi, V. Lomakin and Y. Fainman, "Sub-wavelength semiconductor lasers for dense chip-scale integration," Advances in Optics and Photonics, vol. 6, no. 1, 1-56 (2014)
2. Hill, M. T., Oei, Y.-S. , Smalbrugge, B., Zhu, Y., de Vries, T., van Veldhoven, P. J., van Otten, F. W. M., Eijkemans, T. J., Turkiewicz, J. P., de Waardt, H., Geluk, E. J., Kwon, S.-H., Lee, Y.-H., Nötzel, R., and Smit, M. K., Lasing in mtellic-coated nanocavities. Nature Photon. 1, 589 (2007)
3. Mizrahi, A., Lomakin, V., Slutsky, B. A., Nezhad, M.P., Feng, L., and Fainman, Y., Low threshold gain metal coated laser nanoresonators. Opt. Lett. 33(11) 1261-1263, (2008)
4. Hill, M. T., Marell, M., Leong, E. S. P., Smalbrugge, B., Zhu, Y., Sun, M., van Veldhoven, P. J., Geluk, E. J., Karouta, F., Oei, Y. S., Nötzel, R., Ning, C. Z., and Smit, M. K., Lasing in metal–insulator–metal sub-wavelength plasmonic waveguides. Opt. Express 17, 11107-11112 (2009)
5. Perahia R, Mayer Alegre, T.P., Safavi-Naeini, A.H., Painter, O., Surface-plasmon mode hybridization in subwavelength microdisk lasers. Appl Phys Lett.; 95, 201114 (2009)
6. Nezhad, M. P., Simic, A., Bondarenko, O., Slutsky, B., Mizrahi, A. , Feng, L., Lomakin, V., Fainman, Y., Room-temperature subwavelength metallo-dielectric lasers. Nature Photonics 4, 395 - 399 (2010)
7. Yu, K., Lakhani, A., and Wu, M. C., Subwavelength metal-optic semiconductor nanopatch lasers. Opt. Express 18, 8790-8799 (2010)
8. Lu, C.Y., Chang, S.W., Chuang, S.L., Germann, T.D., Bimberg, D., Metal-cavity surface-emitting microlaser at room temperature. Appl Phys Lett. 96 251101–251103 (2010)
9. K. Ding, Z. Liu, L. Yin, H. Wang, R. Liu, M. T. Hill, M. J. H. Marell, P. J. van Veldhoven, R. Nötzel, and C. Z. Ning, Electrical injection, continuous wave operation of subwavelength-metallic-cavity lasers at 260 K. Appl. Phys. Lett. 98(23), 231108 (2011)
10. Ding, Q., Mizrahi, A., Fainman, Y., Lomakin, V., Dielectric shielded nanoscale patch laser resonators. Opt. Lett. 36, 1812–1814 (2011)
11. Lee, J.H., Khajavikhan, M., Simic, A., Gu, Q., Bondarenko, O., Slutsky, B., Nezhad, M.P., and Fainman F., "Electrically pumped sub-wavelength metallo-dielectric pedestal pillar lasers", Optics Express, 19 (22), 21524-21531 (2011)
12. Ding, K., Liu, Z. C., Yin, L. J., Hill, M. T., Marell, M. J. H., van Veldhoven, P. J., Nöetzel, R.,Ning, C. Z. Room-temperature continuous wave lasing in deep-subwavelength metallic cavities under electrical injection. Phys Rev B 85 041301–041305 (2012)
13. Khajavikhan, M., Simic, A., Katz, M., Lee, J. H., Slutsky, B., Mizrahi, A., Lomakin, V. and, Fainman, Y., "Thresholdless Nanoscale Coaxial Lasers", Nature, 482, 204–207 (2012)
14. K. Ding, M. T. Hill, Z. C. Liu, L. J. Yin, P. J. van Veldhoven, and C. Z. Ning, "Record performance of electrical injection sub-wavelength metallic-cavity semiconductor lasers at room temperature," Opt. Express 21, 4728-4733 (2013)
15. Li, D.B, Ning, C.Z., Peculiar features of confinement factors in a metal–semiconductor waveguide, Appl Phys Lett 96 181109–181111 (2010)
16. L. A. Coldren and S. W. Corzine, Diode Lasers and Photonic Integrated Circuits (John Wiley & Sons, Inc., 1995)

17. Chang, S. W., and Chuang, S. L., Fundamental formulation for plasmonic nanolasers. JQE IEEE, 45 8 1014-1023 (2009)
18. Li, D. B., Ning, C. Z., Giant modal gain, amplified surface plasmon-polariton propagation, and slowing down of energy velocity in a metal–semiconductor–metal structure. Phys Rev B 80 153304–153307 (2009)
19. Björk, G., Karlsson, A. and Yamamoto, Y., Definition of a laser threshold. Phys. Rev. A 50 (2), 1675-1680 (1994)
20. Chi-Yu Adrian Ni and Shun Lien Chuang, "Theory of high-speed nanolasers and nanoLEDs," Opt. Express 20, 16450-16470 (2012)
21. Khurgin, J. B. and G. Sun, Comparative analysis of spasers, vertical-cavity surface-emitting lasers and surface-plasmon-emitting diodes. Nat Photon, 8(6): p. 468-473 (2014)
22. Xu Yang, Ming Xin Li, Guowei Zhao, Sabine Freisem, Dennis G Deppe, Small oxide-free vertical-cavity surface-emitting lasers with high efficiency and high power, Electronics Letters 50, 1864-1866 (2014)
23. http://www.oepic.com/hm021206/index.htm
24. R. Hanbury Brown and R. Q. Twiss, "Interferometry of the intensity fluctuations in light. II. An experimental test of the theory for partially coherent light". Proceedings of the Royal Society A 243 (1234): 291–319 (1958)
25. S. Hartmann, A. Molitor, M. Blazek, and W. Elsäßer, "Tailored first- and second-order coherence properties of quantum dot superluminescent diodes via optical feedback," Opt. Lett. 38, 1334-1336 (2013)